Pakistan Veterinary Journal

ISSN: 0253-8318 (PRINT), 2074-7764 (ONLINE)
DOI: 10.29261/pakvetj/2024.132

RESEARCH ARTICLE

Early Detection of Functional Changes in an Intraocular Hypertension Rabbit Model Treated with Human Wharton Jelly Mesenchymal Stem Cells (hWJ-MSCs) Using Chromatic Pupillometry

Karine dos Santos Evangelho[1], Carlos Cifuentes-González[2], William Rojas-Carabali[2], Clemencia De Vivero-Arciniegas[3], Carlos Téllez-Conti[3], Mariana Cañas-Arboleda[4], Gustavo Salguero[4], Carolina Ramírez-Santana[5] and Alejandra de-la-Torre[2*]

[1]Doctoral Program Biomedical and Biological Sciences, School of Medicine and Health Sciences, Universidad del Rosario, 11121, Bogotá, Colombia
[2]Neuroscience (NEUROS) Research Group, Neurovitae Center for Neuroscience, Institute of Translational Medicine (IMT), Escuela de Medicina y Ciencias de la Salud, Universidad del Rosario, Bogotá, Colombia
[3]Escuela Superior de Oftalmología del *Instituto* Barraquer de América, 11121, Bogotá, Colombia
[4]Advanced Therapies Unit, Instituto Distrital de Ciencia Biotecnología e Innovación en Salud—IDCBIS, 111611 Bogotá, Colombia
[5]Center for Autoimmune Diseases Research (CREA), Institute of Translational Medicine (IMT), School of Medicine and Health Sciences, Universidad del Rosario, Bogotá, 11121, Colombia
*Corresponding author: alejadelatorre@yahoo.com

ARTICLE HISTORY (23-240)

Received:	June 14, 2023
Revised:	December 6, 2023
Accepted:	December 8, 2023
Published online:	February 10, 2024

Key words:
Ocular hypertension
Mesenchymal stromal cells
Chromatic pupillary light reflex
Visual evoked potentials
Early detection.

A B S T R A C T

The present study was designed to evaluate the use of a chromatic pupillometry test for the early detection of functional impairment in intrinsically photosensitive retinal ganglion cells (ipRGCs) in an experimental glucocorticoid model of ocular hypertension (OH) treated with intravitreal injection of human Wharton's jelly derived mesenchymal stromal cells (hWJ-MSCs). For this purpose, fifteen New Zealand rabbits were randomly assigned to three groups: OH (G1), hWJ-MSCs (G2), and OH + hWJ-MSCs (G3). The chromatic pupillary light reflex (cPLR) was assessed after dark adaptation to high-illuminance red and blue light stimuli. Response to blue light was used as a marker of ipRGC activity. Amplitude and latency were evaluated using flash-visual evoked potentials (VEP). Intraocular pressure (IOP) (mmHg) was monitored over time. The results indicated a significant increase ($P<0.001$) in the IOP by third week. Pupil diameter (mm) for blue light significantly increased ($P<0.05$) in all groups compared to the control eyes. However, the pupillary diameter in G3 tended to remain constant. Red light elicited significant differences in the responses in G1 ($P=0.025$) and G2 ($P=0.007$). Moreover, we found no correlation between the parameters of blue light intensity and flash-VEP ($P>0.05$). A non-significant increase in the latency of G2 ($P=0.437$) and G3 ($P=0.779$), and a slight increase in the amplitude of G3 were observed ($P=0.268$). The changes generated by the OH can be recognized early through quantitative measurements of the pupillary function. We found that intravitreal injection of human hWJ-MSCs appears to influence ipRGC activity, detectable early through cPLR in eyes with OH. In summary, our study indicates that intravitreal injection of human hWJ-MSCs appears to influence ipRGC activity facilitating the early detection capabilities for ocular hypertension-related changes through cPLR in eyes with OH.

To Cite This Article: Evangelho KDS, Cifuentes-González C, Rojas-Carabali W, Vivero-Arciniegas CD, Téllez-Conti C, Cañas-Arboleda M, Salguero G, Ramírez-Santana C and de-la-Torre A, 2024. Early detection of functional changes in an intraocular hypertension rabbit model treated with human wharton jelly mesenchymal stem cells (hWJ-MSCs) using chromatic pupillometry. Pak Vet J, 44(1): 29-37. http://dx.doi.org/10.29261/pakvetj/2024.132

INTRODUCTION

Glaucoma, characterized by a loss of the retinal ganglion cells (RGCs) and alterations in the optic nerve, leads to visual impairment (Arrigo *et al.*, 2021). Early detection and treatment of glaucoma are crucial to halt disease progression (Arévalo-López *et al.*, 2023) prompting exploration into neuroprotective therapies to impede the rapid, irreversible cascade of events culminating in blindness (Scott *et al.*, 2013). The chromatic

pupillary response has been considered a potentially sensitive disease biomarker diminishes with damage to intact melanopsin-dependent intrinsically photosensitive retinal ganglion cells (ipRGCs) (Rukmini *et al.,* 2019). Notably, its advantages include ease of application, portability, and cost-effectiveness (Suo *et al.,* 2020). In veterinary medicine, the chromatic pupillary response aids in diagnosing sudden acquired retinal degeneration syndrome (Graham *et al.,* 2020) and optic nerve diseases (Terakado *et al.,* 2013).

However, there is compelling evidence demonstrating the potential for functional restoration in retinal ganglion cells (RGCs) and various neural cell types in several blinding diseases (De Silva *et al.,* 2017; Tang *et al.,* 2018), rendering neuroprotective therapies highly promising.

Mesenchymal stem cells (MSCs) have recently emerged as a promising candidate for treating retinal diseases, including glaucoma (Adak *et al.,* 2021; Vilela *et al.,* 2021). The potential application of MSCs as a neuroprotective therapy for glaucoma stems from their multipotent self-replication, low immunogenicity, ease of isolation and their expansion (Nauta and Fibbe, 2007), and notable paracrine properties (Mead *et al.,* 2016). Cells derived from human Wharton jelly (hWJ), in particular, exhibit higher expression of neurotrophic factors and a spontaneous trend toward neural lineage differentiation compared to other MSC sources (Drela *et al.,* 2016). In this context, hWJ-MSCs have demonstrated electrophysiological properties consistent with mature neurons, similar to observations in bone marrow-derived MSCs (Wislet-Gendebien *et al.,* 2005) suggesting their potential to ameliorate optic nerve damage caused by ocular hypertension (OH) (Johnson *et al.,* 2010).

To detect early damage and functional loss in retinal ganglion cells (RGCs) associated with glaucoma, a widely used technique is visual evoked potentials (VEP). Flash-VEP is a practical and effective diagnostic method that reveals the activity of the visual system at the occipital visual cortex level. The responses obtained from the visual stimulus are represented in a waveform. Measurement of wave latency (the time taken for the signal to travel from the retina to the visual cortex) and amplitude (the indicative of the number of retinal ganglion cells working to activate an electrical signal) are employed to evaluate flash-VEP (Tai, 2018).

Our study aimed to assess the early changes generated by OH in the intrinsically photosensitive retinal ganglion cells (ipRGCs) using Flash-VEP and chromatic pupil light reflex (cPLR), as well as to investigate the impact of hWJ-MSCs therapy on retinal and optic nerve function.

MATERIALS AND METHODS

Animals: All experimental and animal care procedures were conducted in accordance with the Association for Research in Vision and Ophthalmology (ARVO) for the Use of Animals in Ophthalmic and Vision Research and approved by the Animal Ethics Committee (reference C-20190226-1). The study included 15 New Zealand White (NZW) male rabbits aged approximately 4r months and weighing 2–3 kgs. The animals were housed in a controlled environment with 50±20% relative humidity, room temperature of 15-23ºC and 12-hours light / 12-hours darkness cycle. All animals were caged individually and received a standard maintenance diet, water, and hay *ad libitum* once a day.

Before inclusion, each animal underwent a comprehensive ocular examination to exclude the presence of ocular diseases. Ophthalmic examinations included intraocular pressure (IOP) measurement (mmHg) using applanation tonometry (Tono-Pen AVIA Vet™/ Reichert, USA), slit-lamp biomicroscopy of the anterior segment (SL-15/ Kowa, Tokyo, Japan), direct ophthalmoscopy (Welch Allyn, Skaneateles Falls, USA), and indirect ophthalmoscope (Vantage Plus binocular, Keeler, UK). The study comprised three intervention groups, each with five animals: Group 1: ocular hypertension (OH), Group 2: hWJ-MSCs, and Group 3: OH + hWJ-MSCs. The left eye served as the control in all cases, and animals with posterior segment alterations were not included in the study.

Anesthesia procedure: For the intravitreal injection of hWJ-MSCs and flash-VEP, the animals were anesthetized with ketamine (Ketafine®, Brouwer, Argentina) (35 mg/kg) and xylazine (Xilacina 2%, Erma, Colombia) (8 mg/kg) through intramuscular injections. Prior to the subconjunctival glucocorticoid injection, anesthetic eye drops containing 0.5% proparacaine (Alcaine®, Alcon, Barcelona) were administered. To mitigate the potential complications from tropical anesthesia, artificial tears (Splash Tears, Sophia, Colombia) were instilled twice daily, following IOP measurement.

Induction of ocular hypertension: OH was induced in 10 eyes, with 5 eyes each in G1 and G3. Induction involved twice-daily drops of prednisolone acetate (Prednefrin Forte® Eye drops 10 mg/mL – Allergan, Brazil) and weekly subconjunctival injection of 0.5 mL of betamethasone acetate (Celestone Cronodose®, disodium phosphate, 3+3 mg/mL, Schering-Plough, Mexico) in the right eye over a period of five weeks.

Measurements of intraocular pressure: IOP measurements (mmHg) were taken twice daily (at 7:00 a.m. and 4:00 p.m.) for nine consecutive weeks in both eyes of all experimental animals. The tonometer was calibrated according to the manufacturer's instructions and minimal head and neck restraint were applied to avoid excessive pressure on the eyelids and neck. Five readings were averaged for each eye, IOP measurements with repetitions below a 90% confidence level were discarded and re-measured for accuracy. The eye examined first was chosen randomly using an Excel generated sequence. To ensure consistency across animals and groups, the same examiner performed tonometry in all the cases. OH was defined as IOP exceeding above 15mmHg, based on established IOP levels in rabbits (Pereira *et al.,* 2011).

Isolation and culture of hWJ-MSCs: Umbilical cord samples were collected from full-term births including both caesarean and vaginal deliveries (n=5). Informed consent was obtained and approved by the Ethical Committee (reference 2019EE44993). Exclusion criteria for cord donors considered sociodemographic variables such as age,

nutritional status during pregnancy, drug dependence, history of congenital anomalies, congenital immune or metabolic deficiencies, viral infections (including chickenpox, papillomavirus, HIV, among others), bacterial or parasitic infections during pregnancy, eclampsia, and multiple pregnancies.

The umbilical cord samples were handled aseptically and immediately placed in a container with cold physiological saline solution (0.9% NaCl) and stored at 4°C until arrival at the laboratory. Umbilical cord fragments were washed with 0.9% saline solution containing 1% penicillin/streptomycin (10,000U/mL), and the umbilical veins, arteries, and outer membranes were removed. Wharton's jelly was minced and cultured in flasks containing low glucose Dulbecco's Modified Eagle's medium (Gibco, Life Technologies, USA), supplemented with 10% human platelet lysate (hPL plus) and 8 IU/mL of heparin. The hWJ-MSCs cultures were maintained at 37°C in a humidified atmosphere with 5% CO2 with the culture medium replaced every three days. Once hWJ-MSCs reached 80% confluence, they were subcultured for a few passages and used as cell sources in subsequent experiments. Cells were induced to differentiate into adipocytes, osteocytes, and chondrocytes and hWJ-MSCs were expanded to the third passage and used in subsequent experiments.

Characterization of hWJ-MSCs: Cells were immunophenotypically characterized using antibodies against the following human antigens: CD90-APC, CD73-PE/Cy7, CD105-PE, CD274-PE, CD45-APC/Cy7, CD34-PerCP-Cy5.5, and CD31-PE (*Biolegend, San Diego, USA*), following the manufacturer's instructions for dilution. Appropriate isotype controls were applied for each antibody. Inhibition of $TCD3^+$ was assessed, and the cell suspension underwent analysis for sterility, endotoxins, and mycoplasmas. Flow cytometry analyses were performed using a FACSCanto II™ instrument (*BD, Franklin Lakes, USA*) with da analyzed using the FlowJo vX.7.0 software package (*TreeStar, USA*).

Intravitreal injection of hWJ-MSCs: For intravitreal application of hWJ-MSCs, the eyeball was first aseptically cleaned with 5% povidone-iodine, applied a drop of anesthetic, and a disposable surgical drape was spread around the eyeball. Afterwards, using a surgical microscope (Zeiss, Germany) and a blepharostat, the previously thawed hWJ-MSCs suspension ($1x10^5$cells/100µL) was gently injected 4 mm posterior to the lateral corneal limbus, through the sclera to the vitreous cavity in the region of the pars plana with a 30-gauge needle in the direction of the optic disc in G2 and G3 at week seven. The cells were injected cautiously to prevent direct contact with the lens and to avoid damage to the vortex veins, which might induce eye inflammation and cataracts. The injection was administered slowly over approximately 1 minute).

To prevent the escape of the vitreous-applied solution, gentle pressure was applied to the area using a sterile swab for 1 minute. The control eye received an intravitreal injection of sterile balanced salt solution (BSS™ Sterile, Alcon Laboratories). Animals were monitored daily including ophthalmological examinations of the anterior and posterior segments of the eye, during the postoperative period after the procedure.

Chromatic pupil light reflex and pupillometry measurements: The cPLR was measured in both eyes at weeks 1, 3, 6, and 9 using the Precision Illuminator BPI-50 (Retinographics, Inc., USA). Despite, rabbits lacking photoreceptors for red light, we opted to evaluate their response to it. This decision was made considering the presence of blue (430 nm sensitivity) and green (520 nm sensitivity) cones as well as rods in the rabbit retina (De Monasterio, 1978). This choice accounted for potential spectral interactions in retinal neurons. The assessments occurred in a dark room to stimulate the pupillary function at higher levels (10000 lx±5%) using red light (660 nm), and blue light (465 nm). The red-light response was measured within 5 seconds of high-intensity stimulation. After 10-minute adaptation to darkness pupil recovery, the stimulation test was repeated with blue light using the same protocol. Additionally, baseline pupillary measurements were obtained under ambient light conditions before the procedures. Photographs of the eyes were captured for subsequent analysis of the pupillary diameters using ImageJ application (v.1.53e, Wayne Rasband, USA) was used to measure the pupillary diameter. Pupillary constriction was estimated based on the relative diameter of the pupil at the maximum contraction and rest (relative pupil diameter at maximum constriction) / (relative resting pupil diameter) (Fig. 1). All measurements were consistently performed by the same researcher.

Flash-VEP test: Flash-VEP was employed to evaluate the function of the RGCs and visual pathways. All rabbits were examined using the BPM-300 Retinographics ERG/VEP equipment (Retinographics, Inc., USA) following the International Society for Clinical Electrophysiology of Vision (ISCEV) standards for clinical visual evoked potentials in humans. To minimize potential biases in the flash-VEP recordings, parameters such as body temperature, amount of anesthesia used, and location of the recording electrodes in each evaluation were controlled. Examinations were conducted in both eyes at weeks 1 and 9. Before testing, the pupil dilatation was achieved using a 0.5% tropicamide. The eyes were then opened using a blepharostat. Responses were obtained by stimulating only one eye and recording from the active electrode, while the contralateral eye was obstructed to prevent light stimulation. Flash-VEP signals were recorded using a stainless-steel needle as the active electrode, inserted under the skin above the area of the visual cortex midway between the two ears. Reference and ground electrodes were inserted into the ear. We used a time base of: 5ms/Div, sensitivity of 2µV/Div, stimulus single, inter-test time 2s, intensity 3.0cd-s/m², and an average of 64 were given to the right eye. Flash-VEP analysis was based on amplitude (P2) and latency (N2), with both automatically calculated using a computer program after the measurements.

Statistical analyses: The statistical analysis was performed using Jamovi Version 2, presenting results as mean (SD) [IQR]. Normality was assessed using the Shapiro-Wilks test, and for normal distribution, repeated measures ANOVA was employed; otherwise, Friedman

ANOVA. Post hoc tests included Tukey, Bonferroni, Conover, Levene, and Games-Howell based on homoscedasticity. One-way ANOVA or Kruskal-Wallis ANOVA determined differences between groups. Correlation analysis utilized Pearson or Spearman tests. Significance was set at $P<0.05$.

RESULTS

Characterization of hWJ-MSCs: The cultured hWJ-MSCs exhibited a spindle-shaped morphology and adhered to plastic surfaces. Fluorescence-Activated Cell Sorting (FACS) analysis, revealed the positive expression of MSCs markers (CD90, CD73, CD105, and CD274) was positive, while hematopoietic markers (CD45, CD34, and CD31), endothelial marker (CD31), and human leukocyte antigens marker (HLA-DR) were found negative (data not shown). In addition, these cells successfully differentiated into chondrocytes and osteoblasts (data not shown).

The achieved inhibition percentage of $CD3^+$ T cells was found to be ≤87% while, among the utilized total cell concentration $9.58 \times 10^5 \pm 8.88 \times 10^4$ cells/mL/vial, live cell concentration was $9.50 \times 10^5 \pm 8.39 \times 10^4$ cells/mL with a viability of 99.2±0.546% and negative microbiological study.

IOP in an early glaucoma model: The IOP showed a significant increase ($P<0.001$, Kruskal-Wallis ANOVA) in the OH groups from 3rd week of the study (Table 1). Individual analysis revealed significant differences ($P<0.05$) in the OH groups (Supplementary: Table 1, Table 2 and Fig. 1). No significant differences ($P>0.05$) were observed in the control eyes. The maximum IOP values were G1:25.22±12.31[13.0-64.0] mmHg, G2:13.33±3.32 [7.0-25.0] mmHg, and G3:19.16±4.47 [11.0 -42.0] mmHg. Upon suspension of glucocorticoids at week 5, G1 exhibited a sudden increase in IOP compared to G3. Additionally, all groups showed a slightly higher IOP in the afternoon than in the morning, although this difference was not significant, indicating that the animals were adequately acclimatized ($P>0.05$, Kruskal-Wallis ANOVA).

Ophthalmological examination *post* hypertension and hWJ-MSCs application: A complete ophthalmological examination was conducted daily before the induction of ocular hypertension to identify the possible ophthalmological changes produced during the development of the proposed experimental model. When assessing the anterior segment using a slit lamp, no alterations in the corneal curvature or irregularities in the corneal surface were observed with topical anesthesia.

Throughout the five weeks of hypertension induction, no damage to the annexed organs of the eyeball or the presence of blepharospasm, epiphora, or photophobia- indicative of pain or discomfort- were observed in groups G1 and G3. However, starting from week 7 of the study, after the application of hWJ-MSCs, one animal from G3 exhibited intense conjunctival hyperemia, mild corneal edema, rubeosis iridis and iritis, with clinical characteristics changing by week 9 (less conjunctival hyperemia, gray-green iris, and corneal edema). In G2, one animal showed mydriasis without a response to light stimulation at week 9. Following the intravitreal injection of hWJ-MSCs, no posterior segment abnormalities, such as retinal or optic disc issues, were observed in G3.

Baseline pupil size: Analysis of the baseline pupil diameter (mm) showed some differences between the groups (Table 2). G1 exhibited a significant increase in pupillary diameter between weeks 3 and 9 ($P=0.05$, ANOVA; $P=0.160$, Tukey test, and $P=0.345$, Bonferroni test). A similar increase in pupillary diameter was observed in G2 at week 1 compared to week 9 ($P<0.001$; Corrected with Tukey test, and $P=0.002$, Bonferroni); week 3 compared to week 9 ($P=0.004$; $P=0.012$, Corrected with Tukey test, and $P=0.023$, Bonferroni) and week 6 compared to week 9 ($P=0.023$; after adjustment, significance was lost, $P=0.068$, Tukey test, and $P=0.141$, Bonferroni). However, in G3, clear statistical significance was not found in pupillary diameter between weeks in the post hoc analysis. Regarding the analysis of the differences between the groups during the follow-up period, statistically significant differences were only present in week 9 between the G2 and control groups ($P=0.005$, Games-Howell) (Table 3, Fig. 2).

Red light stimulation: In cPLR with red light, significant weekly differences in the pupillary diameter in G1 ($P=0.025$) and G2 ($P=0.007$) were observed. Notably, G2 presented statistically significant differences between weeks 1 and 9 ($P=0.046$; correction loss significance $P=0.131$, Tukey test, and $P=0.161$, Bonferroni).

A significant increase in pupillary diameter was observed in week 3 (Table 4). In addition, the pupillary size in response to the red stimulus was greater in G2 than in the control at week 3 **(**$P=0.039$). Furthermore, G3 demonstrated a significant increase in pupillary diameter in G3 at week 6 compared with that in G2 ($P=0.039$). Finally, statistically significant differences in the relative pupil size were observed between the groups ($P=0.0037$) at week 9. Nevertheless, no significant differences were observed in specific groups in the Games-Howell test (Fig. 2).

Blue light stimulation: The cPLR response to blue light exhibited a significant increase in pupillary diameter in all groups; however, the control group did not show alterations in the pupillary response (Table 5). In G2, there was a significant increase in pupillary diameter between weeks 1 and 9 ($P=0.034$), weeks 3 and 9 ($P=0.004$), and weeks 6 and 9 ($P=0.005$,). Additionally, in G3, significant pupillary alterations were observed between weeks 1 and 3 ($P<0.001$), weeks 1 and 6 ($P=0.007$), and weeks 1 and 9 ($P=0.003$). In contrast, G1 did not show any differences in the Conover test by weeks. (Table 5). In the analysis of differences between the groups, significant variations in the pupillary diameter between all the study groups were observed (Table 6). However, no alterations in pupillary response were found between any group in the post hoc analysis in week one. Large pupillary diameters were noted in G3 than in G2 at week 3 ($P=0.039$, Games-Howell test), in G1 and control ($P=0.039$) at week 6 and in G3 and control ($P=0.011$) at week 6. In comparison to the control, a significant increase in pupil diameter was observed in G2 ($P=0.016$); G3 ($P=0.012$), and G1 ($P=0.053$) at week 9 (Table 6).

Table 1: Analysis of IOP in the different study groups during the study.

IOP	Week 1 Media(SD) [IQR]	Week 2 Media(SD) [IQR]	Week 3 Media(SD) [IQR]	Week 4 Media(SD) [IQR]	Week 5 Media(SD) [IQR]	Week 6 Media(SD) [IQR]	Week 7 Media(SD) [IQR]	Week 8 Media(SD) [IQR]	Week 9 Media(SD) [IQR]
G1	12.8 (2.0) [7.0 - 19.0]	10.5 (2.5) [8.0 - 17.0]	14.3 (2.2) [9.0 - 20.0]	15.1 (2.2) [8.0 - 21.0]	15.5 (3.3) [8.0 - 26.0]	22.0 (7.8) [13.0 - 66.0]	25.2 (12.3) [13.0 - 64.0]	23.8 (14.4) [11.0-74.0]	18.1 (9.9) [12.0-45.0]
G2	12.3 (1.9) [7.0 – 17.0]	11.1 (2.4) [7.0-16.0]	10.8 (1.6) [7.0 – 16.0]	12.0 (1.8) [9.0 – 17.0]	12.9 (1.6) [9.0 – 15.0]	12.3 (3.3) [7.0 – 15.0]	12.7 (2.2) [8.0 – 15.0]	12.2 (1.1) [8.0 – 15.0]	11.6 (1.5) [9.0 – 15.0]
G3	12.2 (2.1) [7.0 – 19.0]	10.2 (3.1) [8.0 – 17.0]	14.2 (3.3) [9.0 – 24.0]	15.3 (3.9) [8.0 - 30.0]	15.2 (4.0) [8.0 - 33.0]	18.2 (3.9) [10.0 - 29.0]	19.2 (4.5) [11.0 - 42.0]	17.2 (4.3) [7.0 – 28.0]	13.2 (3.2) [7.0 – 25.0]

Analysis Kruskal-Wallis ANOVA. G1: ocular hypertension, G2: hWJ-MSCs, G3: ocular hypertension + hWJ-MSCs. Data are presented as mean±SD: Standard Deviation; IQR: Interquartile Range. P<0.05.

Table 2: Analysis of each group's weekly pupil size differences throughout the follow-up time in the baseline light stimulation.

	Baseline pupil size (mm)				
	Week 1 Media (SD) [IQR]	Week 3 Media (SD) [IQR]	Week 6 Media (SD) [IQR]	Week 9 Media (SD) [IQR]	*P*-value
G1	5.7(0.4)[5.2 - 6.0](5 eyes)	5.9(0.9)[5.0 - 7.2](5 eyes)	6.2(0.8)[5.3 - 7.4](5 eyes)	8.0(2.0)[5.4 - 9.6](4 eyes)	0.016*[1]
G2	5.7(0.3)[5.4 - 6.1](5 eyes)	5.8(0.4)[5.3 - 6.2](5 eyes)	5.9(0.6)[5.1 - 6.7](5 eyes)	6.9(0.3)[6.6 - 7.3](4 eyes)	<0.001*[1]
G3	6.0(0.6)[5.3 - 6.9](5 eyes)	6.0(0.9)[5.2 - 7.4](5 eyes)	5.9(0.9)[5.2 - 7.3](5 eyes)	7.1(1.0)[5.4 - 8.2](5 eyes)	0.042*[1]
CONTROL	5.9(0.5)[5.1 - 6.7](15 eyes)	5.8(0.5)[5.1 - 6.6](15 eyes)	5.9(0.6)[4.9 - 6.7](15 eyes)	5.9(0.6)[5.0 - 6.9](14 eyes)	0.994*[1]

Repeated measures ANOVA; [1]Friedman's ANOVA. G1: ocular hypertension, G2: hWJ-MSC, G3: ocular hypertension + hWJ-MSC. Controls of every group correspond to the left eye of the same rabbit. Data are presented as mean±SD: Standard Deviation; IQR: Interquartile Range. mm: millimeters, P<0.05.

Table 3: Analysis of the differences between the groups for each follow-up week, under baseline light stimulation.

	Baseline pupil size (mm)				
TIME DURATION	G1 Media (SD) [IQR]	G2 Media (SD) [IQR]	G3 Media (SD) [IQR]	Control Media (SD) [IQR]	*P*-value
WEEK 1	5.7(0.4) [5.2 – 6.0](5eyes)	5.7 (0.3)[5.4 – 6.1](5 eyes)	6.0 (0.6)[5.3 – 6.9](5 eyes)	5.9 (0.5)[5.1 – 6.7](15 eyes)	0.674[1]
WEEK 3	5.9(0.9)[5.0 – 7.2](5 eyes)	5.8 (0.4)[5.3 – 6.2](5 eyes)	6.0 (0.9)[5.2 – 7.4](5 eyes)	5.8 (0.5)[5.1 – 6.6](15 eyes)	0.981[2]
.WEEK 6	6.2(0.8)[5.3 - 7.4](5 eyes)	5.9 (0.6)[5.1 - 6.7](5 eyes)	5.9 (0.9)[5.2 - 7.3](5 eyes)	5.9 (0.6)[4.9 - 6.7](15 eyes)	0.893[1]
WEEK 9	8.0(2.0)[5.4 - 9.6](4 eyes)	6.9 (0.3)[6.6 - 7.3](4 eyes)	7.1 (1.0)[5.4 - 8.2](5 eyes)	5.9 (0.6)[5.0 - 6.9](14 eyes)	0.011*[1]

[1] One-way ANOVA; [2]Kruskal-Wallis ANOVA. G1: ocular hypertension, G2: hWJ-MSC, G3: ocular hypertension + hWJ-MSC. Controls are a mixed of the three groups. Data are presented as mean±SD: Standard Deviation; IQR: Interquartile Range. mm: millimeters. P<0.05.

Table 4: Analysis of the differences between the groups for each follow-up week under red light stimulation.

	Red pupil size (mm)				
TIME DURATION	G1 Media (SD) [IQR]	G2 Media (SD) [IQR]	G3 Media (SD) [IQR]	Control Media (SD) [IQR]	*P*-value
WEEK 1	5.0(0.8)[4.0 - 5.9](5 eyes)	4.2 (0.6)[3.4 - 4.9](5 eyes)	5.0(1.0)[3.9 - 6.5](5 eyes)	5.1(1.1)[3.4 - 6.9](15 eyes)	0.215[1]
WEEK 3	5.6(1.1)[4.5 - 6.9](5 eyes)	4.6 (0.4)[4.1 - 5.0](5 eyes)	5.5(0.7)[4.5 - 6.3](5 eyes)	5.5(0.9)[3.8 - 6.9](15 eyes)	0.044*[2]
WEEK 6	5.5(1.0)[4.2 - 6.5](5 eyes)	4.6 (0.5)[3.8 - 5.2](5 eyes)	5.6(0.5)[4.9 - 6.1](5 eyes)	5.0(1.2)[3.0 - 6.6](15 eyes)	0.047[1]
WEEK 9	7.2(1.6)[5.2 - 8.8](4 eyes)	6.0 (1.3)[4.7 - 7.8](4 eyes)	6.1(1.0)[4.4 - 6.8](5 eyes)	5.1(0.8)[3.9 - 6.6](14 eyes)	0.037*[2]

[1]One-way ANOVA; [2]Kruskal-Wallis ANOVA. G1: ocular hypertension, G2: hWJ-MSC, G3: ocular hypertension + hWJ-MSC. Controls are mixed of the three groups. Data are presented as mean±SD: Standard Deviation; IQR: Interquartile Range. mm: millimeters. P<0.05.

Table 5: Analysis of the weekly differences in pupil size in each group throughout the follow-up time in the blue light stimulation.

	Blue pupil size (mm)				
	Week 1 Media (SD) [IQR]	Week 3 Media (SD) [IQR]	Week 6 Media (SD) [IQR]	Week 9 Media (SD) [IQR]	*P*-value
G1	2.8(0.3)[2.3 - 3.1](5 eyes)	4.4 (1.7)[2.8 - 7.3](5 eyes)	4.6(1.8)[2.9 - 7.6](5 eyes)	6.0(2.4)[6.0 (2.4)](4 eyes)	0.024*[1]
G2	2.7(0.4)[2.2 - 3.4](5 eyes)	2.7 (0.5)[2.0 - 3.1](5 eyes)	2.7(0.7)[2.1 - 3.8](5 eyes)	4.8(0.4)[4.8 (0.4)](4 eyes)	0.044*[2]
G3	3.1(0.1)[3.0 - 3.2](5 eyes)	4.1 (1.0)[3.4 - 5.8](5 eyes)	3.9(0.9)[3.3 - 5.5](5 eyes)	4.0(0.8)[4.0 (0.8)](5 eyes)	0.014*[2]
CONTROL	2.8(0.4)[2.2 - 3.6](15 eyes)	2.9 (0.4)[2.2 - 3.7](15 eyes)	2.7(0.5)[1.7 - 3.4](15 eyes)	2.8(0.5)[2.8 (0.5)](14 eyes)	0.8[1]

[1]Repeated measures ANOVA; [2]Friedman's ANOVA. G1: ocular hypertension, G2: hWJ-MSC, G3: ocular hypertension + hWJ-MSC. Controls of every group correspond to the left eye of the same rabbit. Data are presented as mean±SD: Standard Deviation; IQR: Interquartile Range. mm: millimeters. P<0.05.

Table 6: Analysis of the differences between the groups for each follow-up week under blue light stimulation.

	Blue pupil size (mm)				
TIME DURATION	G1 Media(SD) [IQR]	G2 Media(SD) [IQR]	G3 Media(SD) [IQR]	Control Media(SD) [IQR]	*P*-value
WEEK 1	2.8 (0.3)[2.3 - 3.1](5 eyes)	2.7 (0.4)[2.2 - 3.4](5 eyes)	3.1 (0.1)[3.0 - 3.2](5 eyes)	2.8 (0.4)[2.2 - 3.6](15 eyes)	0.019*[1]
WEEK 3	4.4 (1.7)[2.8 - 7.3](5 eyes)	2.7 (0.5)[2.0 - 3.1](5 eyes)	4.1 (1.0)[3.4 - 5.8](5 eyes)	2.9 (0.4)[2.2 - 3.7](15 eyes)	0.003*[2]
WEEK 6	4.6 (1.8)[2.9 - 7.6](5 eyes)	2.7 (0.7)[2.1 - 3.8](5 eyes)	3.9 (0.9)[3.3 - 5.5](5 eyes)	2.7 (0.5)[1.7 - 3.4](15 eyes)	0.003*[2]
WEEK 9	6.0 (2.4)[6.0 (2.4)](4 eyes)	4.8 (0.4)[4.8 (0.4)](4 eyes)	4.0 (0.8)[4.0 (0.8)](5 eyes)	2.8 (0.5)[2.8 (0.5)](14 eyes)	<0.001*[2]

[1]One Way ANOVA; [2]kruskal-wallis ANOVA. G1: ocular hypertension, G2: hWJ-MSC, G3: ocular hypertension + hWJ-MSC. Controls are mixed of the three groups. Data are presented as mean±SD: standard deviation; IQR: interquartile range. mm: millimeters. P<0.05.

Amplitude and latency measurements: In the flash-VEP test analysis, a non-significant reduction in N2 (latency) was observed in G1 at week 1 (23.6±10.3 [14.2-40.8] ms), compared to week 9 (13.6±3.7 [10.0-18.2] ms, P=0,491). However, an increase was found in G2 at week 1 (21.9 ±13.3 [11.0-41.5] ms) compared to week 9 (28.3±18.2 [13.0-52.5] ms, P=0.437) and in G3 at week 1 (21.2± 14.4[12.2-42.5] ms), compared to week 9 (21.5±10.7 [10.0-33.2] ms, P=0.779). Latency did not differ significantly between the groups at week 1 (P=0,87) and week 9 (P=0,54). It was observed that the groups which received cell therapy (G2 and G3) exhibited higher latencies compared to the control group, however, the difference was not statistically significant.

In P2 (amplitude), a reduction was observed in G1 at week 1 (18.5±9.9 [5.3-26.9] μv), compared to week 9 (12.6±2.7 [9.8-16.1] μv, P=0.07). However, there were no changes in G2 at week 1 (12.5±4.7 [7.4-18.8] μv), compared

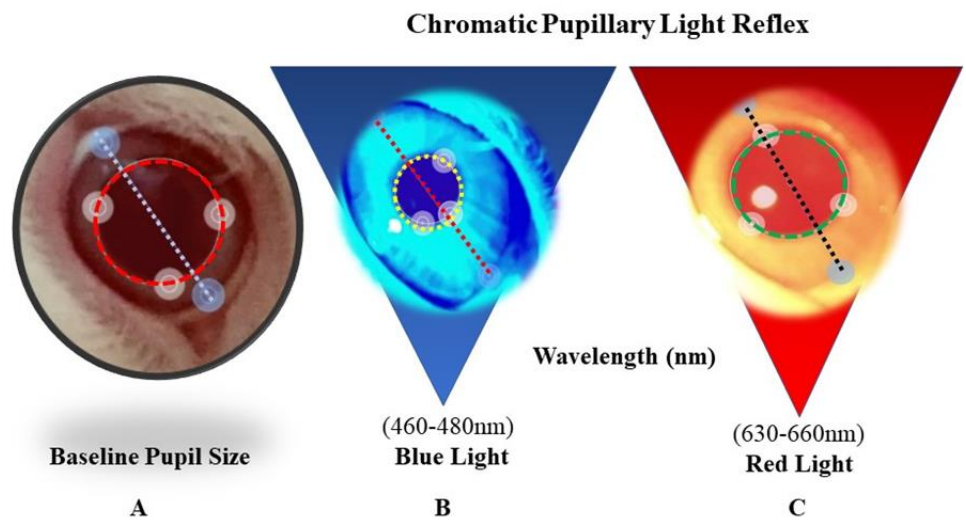

Fig. 1: Pupillary diameter measurement (mm): A line is drawn starting at the lateral limbus and ending at the medial limbus, crossing the central axis of the eye. The pupil is marked by a central line. Pupil diameter is determined by the degree of constriction of the pupil in response to light. **mm:** millimeters. A: Baseline Pupil Reflex, B: Pupillary diameter under blue light, C: Pupillary diameter under red light.

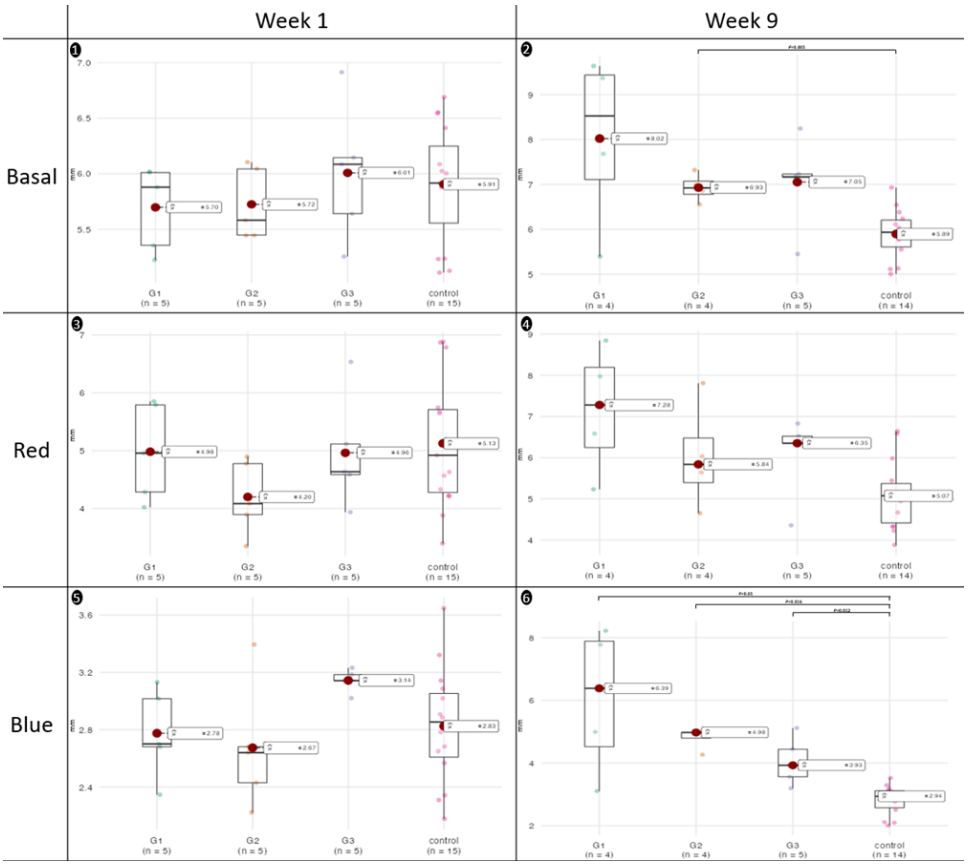

Fig. 2: Chromatic Pupillary Light Reflex. Changes are recorded in pupil diameter during, basal, blue, and red light in the study groups at weeks 1 and 9. Repeated measures ANOVA; Friedman's ANOVA. P<0.05. 1,3,5: eyes week 1 and 2,4,6: eyes week 9. **G1:** ocular hypertension, **G2:** hWJ-MSCs and **G3:** ocular hypertension + hWJ-MSCs

to week 9 (12.6±6.5 [4.1-20.1] µv, P=0.65). Nonetheless, a small increase in G3 at week 1 (10.9±3.3 [7.4-15.4] µv), compared to week 9 (15.2±5.8 [8.0-24.3] µv, P=0.268) was observed. The amplitude did not differ significantly between the groups at weeks 1 (P=0.48) and 9 (P=0.86). Finally, no statistically significant correlations were observed when correlating blue light stimulation with amplitude and latency.

DISCUSSION

Early diagnosis of glaucoma is essential to prevent permanent structural damage and irreversible vision loss. Typically, glaucoma detection relies on examining structural damage to the optic nerve combined alongside measurements of visual function. However, clinical examination of the optic nerve is often subjective and prone to variability. This has led to an increasing demand for research into new objective methods to aid in diagnosing glaucoma (Sharma *et al.*, 2008).

In this study, we developed an ocular hypertension (OH) model capable of inducing rapid changes in retinal function. Furthermore, we demonstrated that cPLR can serve as an early biomarker of the functional changes in ipRGCs induced by this OH model and subsequent cell therapy. To our knowledge, this is the first study to illustrate that intravitreal application of human hWJ-MSCs can impact the diameter of pupillary response, signifying changes in retinal and optic nerve function. However, it may not fully restore retinal function. MSCs secrete growth factors, cytokines, and exosomes, producing regenerative and reparative effects in the microenvironment, potentially explaining the changes in the function of the retina and optic nerve after intravitreal application of hWJ-MSCs (Lai *et al.*, 2010; Tuekprakhon *et al.*, 2021).

Supplementary Table 1: Validation of the ocular hypertension model. Individual analysis of IOP in Group 1 during the study.

Group 1	Week1 Mean(SD) [Range]	Week2 Mean(SD) [Range]	Week3 Mean(SD) [Range]	Week4 Mean(SD) [Range]	Week5 Mean(SD) [Range]	Week6 Mean(SD) [Range]	Week7 Mean(SD) [Range]	Week8 Mean(SD) [Range]	Week9 Mean(SD) [Range]	*P* value
Eye 1	12.8 (1.5) [10.0 - 17.0]	10.6 (2.4) [6.0 - 16.0]	12.0 (2.5) [8.0 - 20.0]	12.9 (1.7) [10.0 - 17.0]	15.1 (3.8) [9.0 - 24.0]	19.1 (2.6) [13.0 - 25.0]	19.2 (2.7) [14.0 - 25.0]	14.6 (2.4) [11.0 - 20.0]	13.2 (0.9) [12.0 - 14.0]	<0.001
Eye 2	11.8 (1.8) [7.0 - 16.0]	8.9 (2.3) [4.0 - 14.0]	10.0 (1.7) [6.0 - 14.0]	11.8 (1.9) [9.0 - 18.0]	14.9 (3.2) [8.0 - 21.0]	20.9 (4.3) [13.0 - 29.0]	21.9 (2.7) [17.0 - 26.0]	NA[NA]	NA[NA]	<0.001
Eye 3	12.6 (2.2) [7.0 - 19.0]	11.8 (1.8) [7.0 - 17.0]	11.3 (1.3) [8.0 - 15.0]	13.2 (2.2) [8.0 - 18.0]	15.2 (3.8) [10.0 - 26.0]	21.3 (2.9) [15.0 - 29.0]	19.4 (2.7) [15.0 - 28.0]	18.3 (2.8) [11.0 - 27.0]	12.5 (0.5) [12.0 - 13.0]	<0.001
Eye 4	12.6 (1.8) [9.0 - 17.0]	11.1 (2.4) [6.0 - 16.0]	11.7 (2.0) [8.0 - 19.0]	14.5 (1.4) [13.0 - 17.0]	17.5 (1.0) [16.0 - 19.0]	30.2 (13.2) [18.0 - 66.0]	45.4 (9.0) [25.0 - 64.0]	46.8 (10.2) [21.0 - 74.0]	34.0 (7.2) [16.0 - 45.0]	<0.001
Eye 5	14.1 (1.9) [8.0 - 19.0]	10.1 (2.4) [5.0 - 14.0]	11.4 (2.5) [5.0 - 18.0]	12.9 (2.5) [10.0 - 21.0]	14.9 (2.8) [11.0 - 26.0]	18.6 (3.3) [13.0 - 27.0]	17.9 (4.3) [13.0 - 33.0]	15.6 (1.7) [12.0 - 20.0]	12.7 (0.5) [12.0 - 13.0]	<0.001

Analysis Kruskal-Wallis ANOVA. Group 1: ocular hypertension. Data are presented as mean±SD: Standard Deviation; IQR: Interquartile Range. P<0.05

Supplementary Table 2: Validation of the ocular hypertension model. Individual analysis of IOP in Group 3 during the study.

Group 3	Week1 Mean(SD) [Range]	Week2 Mean(SD) [Range]	Week3 Mean(SD) [Range]	Week4 Mean(SD) [Range]	Week5 Mean(SD) [Range]	Week6 Mean(SD) [Range]	Week7 Mean(SD) [Range]	Week8 Mean(SD) [Range]	Week9 Mean(SD) [Range]	*P* value
Eye 1	11.5 (2.2) [5.0 - 16.0]	11.1 (2.1) [6.0 - 15.0]	9.4 (2.5) [5.0 - 15.0]	9.8 (1.8) [8.0 - 15.0]	12.7 (2.2) [8.0 - 19.0]	16.1 (3.2) [10.0 - 27.0]	17.8 (4.1) [11.0 - 30.0]	12.0 (3.0) [7.0 - 19.0]	10.5 (1.5) [8.0 - 14.0]	<0.001
Eye 2	12.3 (1.8) [8.0 - 17.0]	10.6 (2.5) [6.0 - 16.0]	11.6 (2.5) [7.0 - 17.0]	13.2 (3.1) [10.0 - 23.0]	13.3 (2.5) [9.0 - 19.0]	17.0 (3.5) [12.0 - 28.0]	16.5 (1.6) [14.0 - 21.0]	16.3 (2.3) [12.0 - 21.0]	11.4 (2.4) [2.0 - 16.0]	<0.001
Eye 3	13.1 (2.5) [7.0 - 18.0]	10.8 (2.5) [6.0 - 17.0]	10.9 (2.0) [8.0 - 15.0]	12.8 (2.7) [8.0 - 18.0]	15.3 (2.9) [10.0 - 23.0]	19.3 (4.0) [14.0 - 28.0]	20.8 (2.8) [15.0 - 26.0]	18.4 (4.2) [11.0 - 27.0]	13.5 (2.3) [10.0 - 19.0]	<0.001
Eye 4	11.9 (2.4) [8.0 - 19.0]	10.0 (2.1) [6.0 - 15.0]	12.3 (1.2) [9.0 - 15.0]	11.9 (1.5) [9.0 - 15.0]	14.0 (2.6) [10.0 - 22.0]	17.1 (3.0) [12.0 - 25.0]	17.4 (1.9) [15.0 - 23.0]	17.6 (2.0) [13.0 - 22.0]	14.0 (2.6) [10.0 - 21.0]	<0.001
Eye 5	12.3 (1.1) [10.0 - 17.0]	10.6 (2.5) [6.0 - 15.0]	13.6 (2.9) [8.0 - 24.0]	18.5 (3.7) [13.0 - 30.0]	20.9 (3.5) [14.0 - 33.0]	21.6 (3.0) [16.0 - 29.0]	23.3 (6.2) [15.0 - 42.0]	21.5 (2.9) [17.0 - 28.0]	16.7 (2.8) [13.0 - 25.0]	<0.001

Analysis Kruskal-Wallis ANOVA. Group 3: ocular hypertension + hWJ-MSCs. Data are presented as mean±SD: standard deviation; IQR: interquartile range. P<0.05

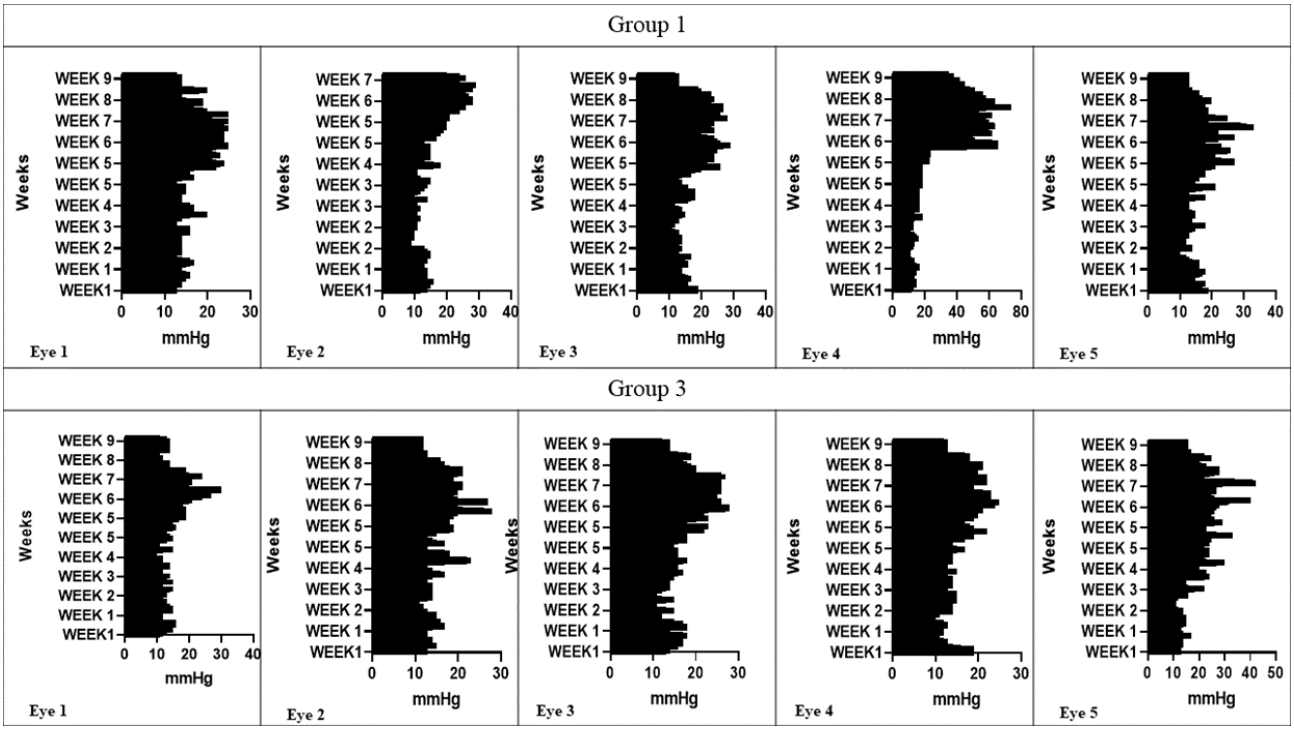

Supplementary Figure 1: Validation of the ocular hypertension model. Individual analysis of IOP in Group 1 and Group 3 during the study. Analysis ANOVA Friedman. Group 1: ocular hypertension. Group 3: ocular hypertension + hWJ-MSCs. IOP: intraocular pressure. IOP measurement: mmHg

Complications typically associated with glaucomatous disease might not manifest in our experimental animal model due to abbreviated research duration in these animals (AlmasiehL and Levin, 2017). Despite inducing OH within short frame, we were able to observe its effects on the optic nerve and retina in the OH group, augmented by hWJ-MSCs. According to a study, changes in rabbit retinas can be detected just four days after applying human MSCs in the vitreous (Xuqian *et al.*, 2011). In our study, these changes were detected early in the cPLR. Similar findings have been reported in the literature for an OH model, showing reduced pupillary responses to blue and red light intensities (Najjar *et al.*, 2018). Interestingly, when evaluating responses to red light, we observed an increase in pupillary diameter in all the study groups, although it was not significant in the OH group that received cell therapy. Since rabbits only possess S and M cones, and lack L cones (responsible for the response to red

light), this finding suggests interactions with other wavelengths (De Monasterio, 1978; Soukup *et al.*, 2019).

As reported in the literature, deficiencies in pupillary responses to blue light were observed in the OH groups compared to non-intervened eyes (Najjar *et al.*, 2018). Moreover, the OH group that received hWJ-MSCs exhibited tendency to maintain a consistent pupillary diameter in response to the intensity of blue light after cell therapy application unlike the group without therapy. This observation in cPLR can be attributed to the ability of RGCs and other neuronal cell types survive for extended periods after disturbances, allowing them to respond to light stimuli (Lin *et al.*, 2008). The observed effect on pupil diameter following hWJ-MSCs application could indicate a possible neuroprotective effect of cell therapy on the retina. An incidental finding revealed a trend towards an altered pupillary diameter in the group that received the cell transplant without OH (a smaller pupillary diameter was observed in the control group than in G2). This phenomenon may be linked to the activation of the intraocular immune response and the release of cytokines and inflammatory mediators the xenotransplantation (Taylor, 2009).

In early glaucoma, an increased latency was observed in the VEP test. This alteration, occurring prior to apoptosis serves as aa potential indicator of functional damage in RGCs (Tai, 2018). Latency measurement can indicate when RGCs are at risk, prompting the need for early intervention to avoid irreversible cell damage. By using the intravitreal route, positioned directly adjacent to the RGCs layer, we hypothesized enhanced neuroprotection with cell therapy. The neuroprotective effects of hWJ-MSCs-induced neuroprotection are linked to their intrinsic characteristics, , which include secret neurotrophic factors that improve the functional integrity of RGCs connections (Mead *et al.*, 2013). Additionally, the intravitreal route of administration requires a smaller volume of applied cells compared to systemic application (Nomura *et al.*, 2005). However, our results for flash-VEP did not show a functional improvement in the latency of animals that received cell transplantation, aligning with the findings described by Vilela *et al.* (2021). Two possible explanations for our observations are: 1) the intravitreal application of stromal cells may not be completely innocuous; or 2) the increased expression in glial fibrillary acidic protein (GFAP) might induce axonal regeneration, leading to metabolic dysfunction and electrophysiological disturbance of neurons (Vázquez-Chona *et al.*, 2011). However, we observed an increase in amplitude in the OH group treated with stem cells, demonstrating potential beneficial effects on RGCs, as described by our cPLR findings.

Throughout the experiment, we did not observe significant differences in latency and wave amplitude measurement between the flash-PEV groups. The influence of small sample size on cell therapy results should be acknowledged, as this can reduce the statistical power. Indeed, studies with a larger number of eyes have reported statistically significant outcomes. However, drawing conclusions about the effect these cells have on the retina's electrical response is challenging. Previous studies have reported that intravitreally injected cells may obstruct the passage of light to the eye by covering the back of lens, thereby altering the electrophysiological analysis (Ezquer *et al.*, 2016). Therefore, further research is required to fully understand this effect.

The combination of cPLR and electrophysiological methods that measure both the function of the optic nerve and the brain response to visual stimuli in rabbits carried out with the RetinoGraphics device in experimental models of glaucoma early have not been previously employed., This poses challenges in comparing our results with existing studies, as data interpretation depends on various factors, including the distance from the light stimuli, the temperature of the animal, and the specific protocol utilized (Firan *et al.*, 2020).

Conclusions: Our study reveals that: 1) the changes induced by OH can be recognized early using the cPLR technique, offering potential benefits for the detection and monitoring of glaucoma; 2) transplantation of umbilical cord hWJ-MSCs can have an impact on ipRGCs, discernable through early measurements of the pupillary diameter; and 3) minimal changes in retinal and optic nerve function were observable through cell therapy. This study contributes to the growing body of research showcasing the potential use of cell therapies in neurodegenerative diseases and provides insights in the early diagnosis of glaucoma for potential clinical applications. However, further research into the role of hWJ-MSCs within the cellular microenvironment post-transplantation is essential to investigate the long-term effects of cell therapy and understand the specific mechanisms underlying pupillary responses in glaucoma patients. Future studies hold the promise of deepening our understanding of glaucoma pathogenesis and advancing innovative treatment approaches.

Authors' contribution: KSE: conceived, designed, performed the experiments, and wrote the manuscript; CHCG: contributed analysis tools and wrote the manuscript; WRC: contributed analysis tools and wrote the manuscript; CVA and CTC: conceived and performed the experiments; MCA and GS: contributed reagents and materials; CRS: wrote the manuscript and Alejandra de-la-Torre: conceived, designed, performed the experiments and wrote the manuscript.

Acknowledgments: We would like to express our sincere gratitude to the Universidad del Rosario, Colombia, and Escuela Superior de Oftalmología del Instituto Barraquer de América, Colombia for their support in this project.

REFERENCES

Adak S, Magdalene D, Deshmukh S *et al.*, 2021. A review on mesenchymal stem cells for treatment of retinal diseases. Stem Cell Rev Reports 17:1154–1173.

AlmasiehL M and Levin LA, 2017. Neuroprotecti on in Glaucoma: Animal models and clinical trials. Annual Rev Vision Sci 3:91–120.

Arévalo-López C, Gleitze S, Madariaga S, *et al.*, 2023. Pupillary response to chromatic light stimuli as a possible biomarker at the early stage of glaucoma: a review. Int Ophthalmol 43:343–356.

Arrigo A, Aragona E, Saladino A, *et al.*, 2021. Cognitive dysfunctions in Glaucoma: An overview of morpho-functional mechanisms and the impact on higher-order visual Function. Front Aging Neurosci 13:747050.

De Monasterio FM, 1978. Spectral interactions in horizontal and ganglion cells of the isolated and arterially perfused rabbit retina. Brain Research 150:239–258.

De Silva SR, Barnard AR, Hughes S, *et al.*, 2017. Long-term restoration of visual function in end-stage retinal degeneration using subretinal human melanopsin gene therapy. Proc Natl Acad Sci USA 114:11211–11216.

Drela K, Lech W, Figiel-Dabrowska A, *et al.*, 2016. Enhanced neuro-therapeutic potential of Wharton's Jelly–derived mesenchymal stem cells in comparison with bone marrow mesenchymal stem cells culture. Cytotherapy 18:497–509.

Ezquer M, Urzua CA, Montecino S, *et al.*, 2016. Intravitreal administration of multipotent mesenchymal stromal cells triggers a cytoprotective microenvironment in the retina of diabetic mice. Stem Cell Res Ther 7:42.

Firan AM, Istrate S, Iancu R, *et al.*, 2020. Visual evoked potential in the early diagnosis of glaucoma. Literature review. Rom J Ophthalmol 64:15–20.

Graham KL, McCowan CI and White A, 2020. Protocol for assessment of the pupillary light reflex in dogs without chemical restraint: preliminary investigation. J Small Animal Prac 61:637–643.

Johnson TV, Bull ND, Hunt DP, *et al.*, 2010. Neuroprotective Effects of Intravitreal Mesenchymal Stem Cell Transplantation in Experimental Glaucoma. Invest Opthalmol Vis Sci 51:2051.

Lai RC, Arslan F, Lee MM, *et al.*, 2010. Exosome secreted by MSC reduces myocardial ischemia/reperfusion injury. Stem Cell Res 4:214–222.

Lin B, Koizumi A, Tanaka N, *et al.*, 2008. Restoration of visual function in retinal degeneration mice by ectopic expression of melanopsin. Proc Natl Acad Sci USA 105:16009–16014.

Mead B, Logan A, Berry M, *et al.*, 2013. Intravitreally transplanted dental pulp stem cells promote neuroprotection and axon regeneration of retinal ganglion cells after optic nerve injury. Invest Ophthalmol Vis Sci 54:7544–7556.

Mead B, Hill LJ, Blanch RJ, *et al.*, 2016. Mesenchymal stromal cell–mediated neuroprotection and functional preservation of retinal ganglion cells in a rodent model of glaucoma. Cytotherapy 18:487-96.

Najjar RP, Sharma S, Atalay E, *et al.*, 2018. Pupillary Responses to Full-Field Chromatic Stimuli Are Reduced in Patients with Early-Stage Primary Open-Angle Glaucoma. Ophthalmology 125:1362–1371.

Nauta AJ and Fibbe WE, 2007. Immunomodulatory properties of mesenchymal stromal cells. Blood 110:3499–3506.

Nomura T, Honmou O, Harada K, *et al.*, 2005. I.v. infusion of brain-derived neurotrophic factor gene-modified human mesenchymal stem cells protects against injury in a cerebral ischemia model in adult rat. Neuroscience 136:161–169.

Pereira FQ, Bercht BS, Soares MG, *et al.*, 2011. Comparison of a rebound and an applanation tonometer for measuring intraocular pressure in normal rabbits. Vet Ophthalmol 14:321–326.

Rukmini AV, Milea D and Gooley JJ, 2019. Chromatic pupillometry methods for assessing photoreceptor health in retinal and optic nerve diseases. Front Neurol 10.

Scott EM, Boursiquot N, Beltran WA, *et al.*, 2013. Early histopathologic changes in the retina and optic nerve in canine primary angle-closure glaucoma. Vet Ophthalmol 16:79–86.

Sharma P, Sample PA, Zangwill LM, *et al.*, 2008. Diagnostic Tools for Glaucoma Detection and Management. Surv Ophthalmol 53:S17.

Soukup P, Maloca P, Altmann B, *et al.*, 2019. Interspecies variation of outer retina and choriocapillaris imaged with optical coherence tomography. Invest Ophthalmol Vis Sci 60:3332–3342.

Suo L, Zhang D, Qin X, *et al.*, 2020. Evaluating state-of-the-art computerized pupillary assessments for glaucoma detection: A systematic review and meta-analysis. Frontiers in Neurology 11.

Tai TYT, 2018. Visual evoked potentials and glaucoma. Asia-Pacific J Ophthalmol 7:352–355.

Tang J, Qin N, Chong Y, *et al.*, 2018. Nanowire arrays restore vision in blind mice. Nat Commun 9:786.

Taylor AW, 2009. Ocular immune privilege. Eye 23:1885–1889.

Terakado K, Yogo T, Nezu Y, *et al.*, 2013. Efficacy of the use of a colorimetric pupil light reflex device in the diagnosis of fundus disease or optic pathway disease in dogs. J Vet Med Sci 75:1491–1495.

Tuekprakhon A, Sangkitporn S, Trinavarat A, *et al.*, 2021. Intravitreal autologous mesenchymal stem cell transplantation: a non-randomized phase I clinical trial in patients with retinitis pigmentosa. Stem Cell Res Therapy 12:52.

Vázquez-Chona FR, Swan A, Ferrell WD, *et al.*, 2011. Proliferative reactive gliosis is compatible with glial metabolic support and neuronal function. BMC Neurosci 12:1–11.

Vilela CAP, Messias A, Calado RT, *et al.*, 2021. Retinal function after intravitreal injection of autologous bone marrow-derived mesenchymal stromal cells in advanced glaucoma. Doc Ophthalmol 143:33–38.

Wislet-Gendebien S, Hans G, Leprince P, *et al.*, 2005. Plasticity of cultured mesenchymal stem cells: switch from nestin-positive to excitable neuron-like phenotype. Stem Cells 23:392–402.

Xuqian W, Kanghua L, WeiHong Y, *et al.*, 2011. Intraocular transplantation of human adipose-derived mesenchymal stem cells in a rabbit model of experimental retinal holes. ORE 46:199–207.